Journal of New Materials for Electrochemical Systems 13, 253-259 (2010)

Tungsten Effect Over Co-hydrotalcite Catalysts to Produce Hydrogen from Bio-ethanol

J.L. Contreras[1,*] , M.A. Ortiz[1], G.A. Fuentes[2] , R. Luna[1], J. Salmones[3], B. Zeifert[3], L. Nuno[1] and A.Vazquez[4]

[1]Universidad Autónoma Metropolitana-Azcapozalco Depto. de Energía, CBI,
Av. Sn.Pablo 180 Col.Reynosa, Azcapotzalco C.P.02200 México D.F., México.
[2]Universidad Autónoma Metropolitana-Iztapalapa, Depto. de IPH, CBI,México, D.F., México
[3]Instituto Politécnico Nacional, ESIQIE,Unidad Prof. ALM, México, D. F., 07738, México
[4]Instituto Mexicano del Petróleo, Eje Central 152, México, D.F.México.

Received: November 10, 2009, Accepted: February 04, 2010

Abstract: *A great stabilization effect of tungsten over the Co-hydrotalcite catalysts to produce H_2 from ethanol in steam reforming was found. The catalysts were characterized by N_2 physisorption (BET area), X-ray diffraction, Infrared ,Raman and UV-vis spectroscopies. Catalytic evaluations were performed in a fixed bed reactor using a water/ethanol mol ratio of 4, at 450°C, and the W concentration studied was from 0.5 to 3 wt%. As W concentration increases, the intensity of crystalline reflections of the Co-hydrotalcite catalysts decreases. There were found porous with the shape of parallel layers with a monomodal mesoporous distribution. Superficial chemical groups as: -OH, H_2O, Al-OH, Mg-OH, W-O-W and CO_3^{2-} were found by infrared spectroscopy. Catalyst with low amounts of W (1%) showed both, the highest H_2 production and the best catalytic stability. The smallest pore volume of this catalyst could be related with long residence times of ethanol in the pores. Tungsten promoted the conversion for the Co-hydrotalcite catalysts. The reaction products were: H_2, CO_2, CH_3CHO, CH_4 and C_2H_4 and the catalysts did not produce CO.*

Keywords: Hydrogen, Pt, WOx,Co-Hydrotalcite, Ethanol

1. INTRODUCTION

Ethanol possesses diverse advantages over the derived hydrocarbons from fossil sources: it is a renewable source and neutral with respect to emissions of CO_2, it is less toxic; it can be more easily stored and without handling risk and it can be obtained in large quantities from biomass; in comparison with methanol and the gasoline[1-2]. In order to produce hydrogen and its potential use in fuel cells, it has been proposed the bio-ethanol as a renewable source using the catalytic steam reforming.

The reaction of ethanol with steam is strongly endothermic and it only produces H_2 and CO_2 if the ethanol reacts in the most desirable way. However, other undesirable products as CO and CH_4 are also formed during the reaction [1]. Other reactions occur such as dehydrogenation of ethanol to CH_3CHO, dehydration to $CH_2=CH_2$, decomposition to CO and CH_4 or CO_2, CH_4 and H_2. The CH_3CHO and the $CH_2=CH_2$ are intermediary products that could be formed during the reaction at relatively low temperatures before the formation of H_2 and CO_2 and finally the formation of coke in the surface of the catalyst.

In this type of reaction, the production of CO and CO_2 is very low, since the reaction produce hydrogen [3-4]. An energetic analysis has shown that only the 30% of total energy is required to produce hydrogen using the ethanol steam reforming [5].

Hydrotalcites are materials consisting of positively charged two-dimensional sheets with water and exchangeable charge-compensation anions in the interlayer region. The nature of both the layer cations and the interlayer anions can be changed and when it occurs, the compounds are known as hydrotalcite-like compounds. They have the general molecular formula $[M_{1-x}^{2+}M_x^{3+}(OH)_2]^{x+}$ $(A_{x/n}^{n-})$ mH_2O where: M^{2+} and M^{3+} are divalent and trivalent metal cations in the brucite-type layers respectively, A^{n-} is the interlayer charge-compensating n-valent anion, x is the molar ratio of $M^{III}/(M^{II} + M^{III})$ and can take values from 0.1 to 0.5 and m is the water of crystallization [6]. We have studied the hydrotalcites because they have a high surface area, a good basic site distribution, and a memory effect [7-9]. The addition of W to hydrotalcite is interesting because the addition of this metal to Pt/Al_2O_3 catalysts has shown a high stability [10]. Besides this, the

*To whom correspondence should be addressed: Email: jlcl@correo.azc.uam.mx
Phone: 53189065 ext 116 , fax 53947378

addition of metallic Co catalyzes the ethanol cracking of the C-C and C-H bonds to produce hydrogen [11-13].

2. EXPERIMENTAL SECTION

2.1. Catalysts Preparation

The hydrotalcites were prepared by precipitation using two salt solutions as precursors. First, in a stirred reactor a salt solution of $Mg(NO_3)_2$ and $Al_2(NO_2)_3$ (J.T. Baker) with a molar ratio of 2 was made. A second solution of Na_2CO_3 (5%) and NaOH (pH = 10) (Carlo Erba) was prepared. These two solutions were mixed drop by drop in a third stirred reactor using water as solvent (60 drops/min) at 60°C in a simultaneous manner having an atomic ratio of Mg^{2+}/Al^{3+} of 1.55, then $Co(NO_3)_2$ was added to get a constant amount of 1 wt%Co. The precipitate was washed, dried and calcined at 450°C for 5 h (sample HTC). Several solids were impregnated with $(NH_4)_{12}W_{12}O_{41}5H_2O$ (Aldrich) having different W concentrations: 0.5 (HTC05W), 1 Co(HTC1W), 2 Co(HTC2W) and 3 wt%W (HTC3W). After this impregnation, the solid was stirred during 24 h at 60°C. This solid was washed, dried at 120°C for 24 h , calcined at 450°C during 5 h and finally H_2 reduced at 450°C.

2.2. Catalysts Characterization

The solids obtained were characterized by X-ray diffraction (XRD) in a Phillips X´ Pert instrument; The XRD patterns of the samples after calcination were obtained using the CuK_α radiation. Diffraction intensity was measured in the 2θ range between 5 and 70° with a 2θ step of 0.02° with 8 seconds per point, the samples were analyzed directly at room temperature. The infrared spectroscopy was performed in a Perkin Elmer spectrophotometer (Spectrum-RX). An infrared beam was sent through a wafer of the sample. The wavenumber range was from 4000 to 400 cm^{-1} and the number of averaged scans was 50. N_2 physisorption at - 192°C was developed in a Micromeritics 2000 instrument. Each sample was pretreated at 200°C under vacuum (1×10^{-4} torr). The diffuse reflectance UV-visible spectroscopic analysis (UV-vis) of the samples was made in a Varian (Cary 5E) spectrophotometer. The range of wavelength was from 3000 to 200 nm.

2.3. Catalytic Tests

The catalytic reaction was made in a U-shaped stainless steel fixed bed reactor. The catalyst (1g, 100 US mesh) was charged for each of the reaction evaluations. The feed of the reactants involved a gaseous mixture of ethanol (Aldrich), water as steam and N_2 (purity 99.99%, Infra-Air Products) and this mixture was supplied by a micrometric needle valve (1 ml/s). A constant mixture of H_2O and CH_3CHOH (molar ratio of 4/1) carried by a N_2 stream was supplied in gas flow using two glass saturators and this mixture was vaporized and kept at 92°C before it was fed to the reactor. The samples were previously reduced in a mixture of gas of H_2/Ar at 450°C. The temperature of the catalyst was raised at 450°C in flow of N_2 for 30 min to activate the catalyst and then the flow of reactants started at 450°C. The catalyst was held at that temperature for 30 min in order to have three analyses and for deactivation tests the catalysts were evaluated during 420 min.

Table 1. Surface area (BET) and W concentration of WOx/Co-Hydrotalcite catalysts.

Catalyst	W (% wt)	Surface Area BET (m^2/g)	Pore volume (cm^3/g)	Pore diameter (Å)
HTC	0	258	0.86	474
HTC05W	0.5	202	0.68	471
HTC1W	1	173	0.47	571
HTC2W	2	187	0.53	583
HTC3W	3	181	0.51	578

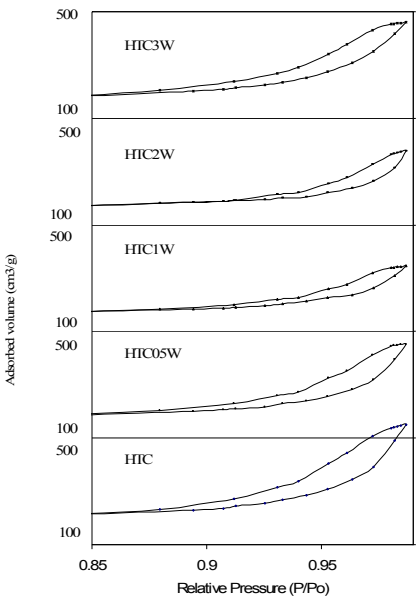

Figure 1. N_2 Hysteresis for WOx/Co-hydrotalcite catalysts

The analysis of the reactants and all the reaction products was carried out online by gas chromatography. Inside an automated injection valve, the sample was divided into two portions which were then analyzed in a different way in order to obtain accurate, complete quantification of the reaction products. One of the portions was used to analyze H_2, CO, CO_2 and CH_4, using a packet column of silica gel 12 grade 60/80 (18´× 1/8") with a thermal conductivity detector (Gow-Mac apparatus). The second portion was used to analyze CH_3CH_2OH, CH_3CHO, CH_3COCH_3, CH_2O and $CH_2{=}CH_2$ with a capillary column (VF-1ms, 15m × 0.25 mm) in a Varian chromatograph CP-3380 with a flame ionization detector (FID). Response factors for all products were obtained and the system was calibrated with appropriate standards before each catalytic test. The conversion (X) was calculated using the ethanol composition before and after of the reaction. The selectivity of each product was defined as follows: Si (%) = Ni / Σ Nj x 100 where: Si(%) is the selectivity of the product i, Ni are the moles of product i, and Nj are the moles of each product (included i).

3. RESULTS AND DISCUSSION

3.1. Textural properties

The surface area BET and the nominal content of W are shown in Table 1. These samples were mesoporous [7] and they showed the hysteresis of the IV type (Figure 1) in accordance with the IUPAC classification [14]. At low pressures, first an adsorbate

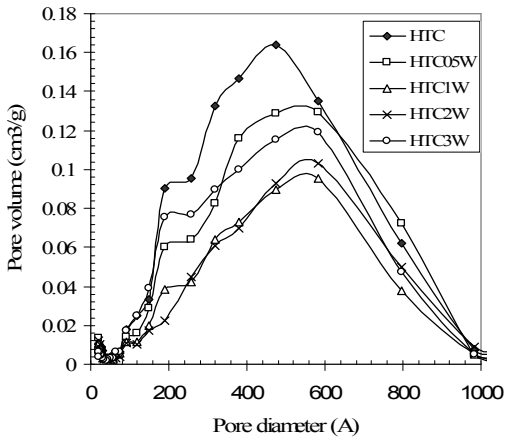

Figure 2. Pore volume and pore diameter of WOx/Co-hydrotalcite catalysts.

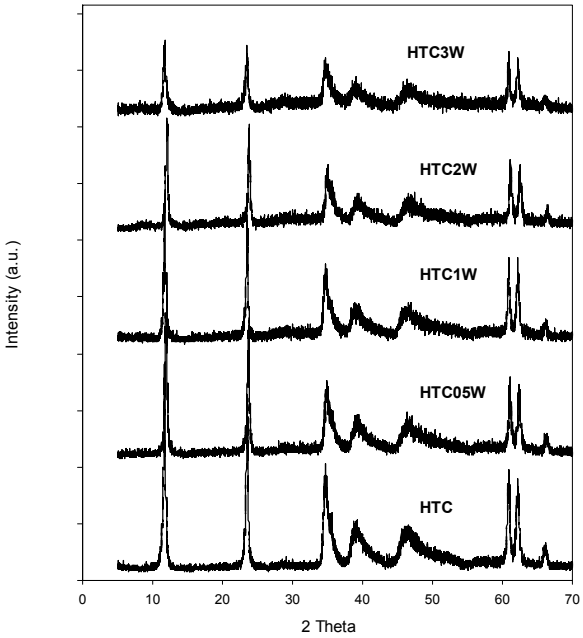

Figure 3. XRD of the WOx/Co-hydrotalcite catalysts

monolayer is formed on the pore surface, which is followed by the multilayer formation. The hysteresis or the isotherms corresponded with the parallel plate structure typical of the hydrotalcites [15]. The surface area obtained for the samples decreased with the W concentration and it was almost the same between HTC2W and HTC3W samples, the pore distribution in Figure 2 shows a monomodal distribution, and the pore volume decreases with the presence of W ions. Co-hydrotalcite sample free of W (sample HTC) showed a wide pore distribution (50 to 1000 Å) which remained for all the samples with W. As W^{6+} ions increased the maximum of pore diameter increased from 474 Å for sample HTC to 578 Å for the sample HTC3W.

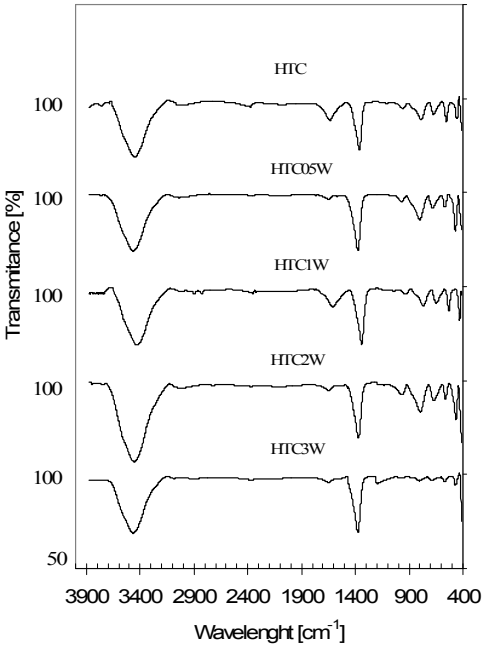

Figure 4. Infrared spectra of the WOx/Co-hydrotalcite

3.2. XRD analysis

For samples with Co, symmetric intense peaks were found in reflections 2θ located in (003), (006), (110) and (113) (Figure 3). Additionally asymmetric peaks with less intensity were found in (012), (015) and (018). These peaks correspond with a laminar structure typical of hydrotalcites [16,17]. As W concentration increased the crystalline structure of the samples decreased and the absence of other phases suggested that both W^{6+} and Co have isomorphically replaced the Mg^{2+} cations in the brucite($Mg(OH)_2$)-like layers [7,11,15]. This effect indicated that the population of structures as the Mg-Al-hydrotalcite decreased, and this behavior has been previously observed with Ni [7].

3.3. Infrared spectroscopy

The infrared spectra for the samples with Co are shown in Figure 4. They showed a broad OH stretching band in the region 3400-3000 cm^{-1} and the H_2O scissoring mode band near 1600 cm^{-1} which provide evidence of the presence of water molecules. Other authors have attributed the band at 3410 cm^{-1} with hydroxil groups coordinated with Mg and Al while the vibration of the same group associated with water is a wide band between 3650-3590 cm^{-1} [18]. A strong band located at 1380 cm^{-1} is attributed to the presence of residual nitrate ions. In the region below 1000 cm^{-1} the spectrum showed a band located in 772 cm^{-1} which are related with vibrations of –OH bending of brucite ($Mg(OH)_2$) type layers [18]. The bands located at 680 and 560 cm^{-1} are related with vibration modes of brucite type layers, specifically with the metal-oxygen symmetrical stretching. The antisymmetric OH stretching band located at 3460 cm^{-1} of the brucite type layers did not change as W concentration increased. Bands located at 790 and 668 cm^{-1} are related with the presence of isopolytungstates. The bands at 786 and 669 cm^{-1} are related with the edge-sharing of W-O-W [15].

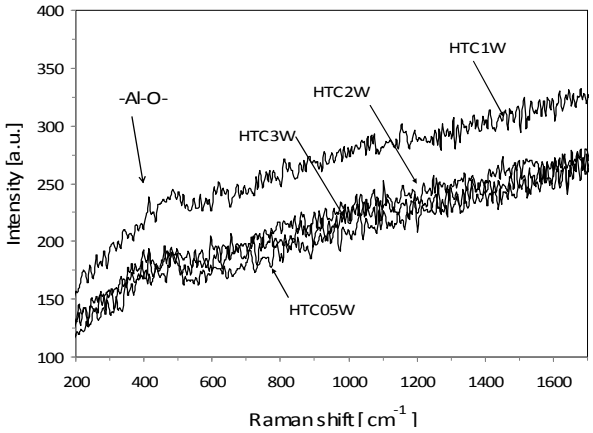

Figure 5. Raman spectra of the WOx/Co-hydrotalcite

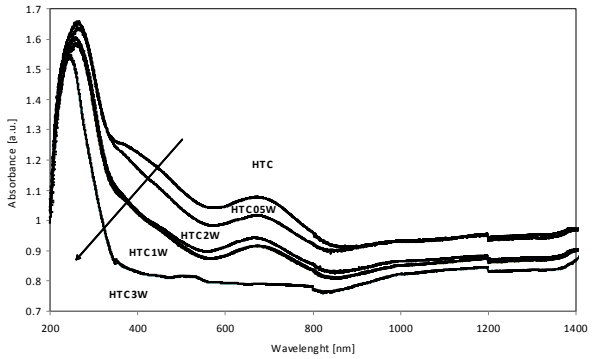

Figure 6. UV-Vis spectra of the WOx/Co-hydrotalcite catalysts

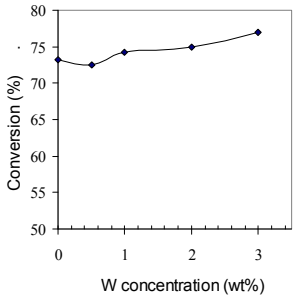

Figure 7. W Effect over the ethanol steam conversion for Co-hydrotalcite catalysts at 450°C (after 7h).

3.4. Raman spectroscopy

The Raman spectra for the samples with Co are shown in Figure 5. It was found a small band located at 490 cm^{-1} which could be related with the -Al-O bending mode of the hydrotalcite. We did not find the band located at 950-1050 cm^{-1} related with octahedral structures of WOx which usually is found on Al_2O_3 [18]. Most of the highest frequency of Raman bands for tetrahedral and octahedral tungsten oxide compounds are between 740 and 1060 cm^{-1} [19], for example the highest frequency for the WO_3 is 805 cm^{-1}, for $Al_2(WO_4)_3$ is 1060 cm^{-1}, for Na_2WO_4 is 928 cm^{-1} and for $(NH_4)_{12}W_{12}O_{41}$ is 980 cm^{-1}. For $[W_{12}O_{42}]^{12-}$ supported on Al_2O_3 the mayor Raman bands are located at 977, 963 and 166 cm^{-1} [20] with the lowest band position attributed to the W-O-W deformation mode. For W compounds, we did not find any Raman bands near 500 cm^{-1}. But the band at 500 cm^{-1} is very close to the position of the strongest band related with the Al-O- bending mode in zeolite A located at 494 and 415cm^{-1}[19].

3.5. UV-vis analysis

The UV-vis spectra for the samples with Co are shown in Figure 6. In the case of Co catalysts, it was found a strong band at 250-270 nm, a wide band between 330-550 nm and the third band located between 550-850 nm (Figure 6). The first band has been attributed to a ligand-metal charge transfer (LMCT) of the single ligand of the W=O [21, 22, 16]. Usually this band increased as the W concentration increased on Al_2O_3 and the W^{6+} was present in a tetrahedral coordination [23-25]. It is know that the structure of tungstated ion $[W_{12}O_{41}]^{12-}$ in aqueous solution is highly dependent of the pH [26] and in alkaline solutions the W^{6+} is present as a tetrahedral monomeric ion $[WO_4]^{2-}$. In this region, it is known that charge transfer transitions involve more than one atom and include transitions from metal to ligand or vice versa, or between two neighboring metal atoms of different oxidation state. In the Figure 6, the absorbance of the spectrum of Co^{2+}/hydrotalcite (sample HTC) decreased as W^{6+} ions were present, so Co^{2+} was substituted by W^{6+} ions. The second band is a d-d band and it could be related with d-d band transitions of tetrahedral Co^{2+} [27]. This band again decreased as the W^{6+} ions increased and the presence of these tetrahedral Co^{2+} species decreased. The third band is again a d-d band related with a weak absorption by octahedral Co^{2+} ion at about 500 nm[27]. This band also decreased as W increased and it seemed that octahedral Co^{2+} species were substituted by W^{6+} ions.

3.6. Catalytic activity

The conversion was defined as percentage of the moles of ethanol converted to products respect to the moles of ethanol fed to the reactor. As W concentration increased the conversion of ethanol increased at 450°C. It was found a W promoter effect in the conversion for these Co/hydrotalcite catalysts (Figure 7). These catalysts produced the following products of reaction: H_2, CH_3CHO, CO_2, CH_4, $CH_2{=}CH_2$ and they did not produce:CH_3COOH, $CH_3CH{=}CH_2$ or other oxygenates, this product distribution was similar with that reported in the literature [11]. Figure 8 shows that H_2 production decreases from HTC1W to HTC3W and increases from HTC to HTC1W, this last catalyst showed the maximum selectivity to H_2.

The experimental results of the Co-hydrotalcite without W (HTC) showed catalytic activity of ethanol steam reforming. Also this type of Co-hydrotalcite has showed activity in other studies [11,16]. The formation of different species on the surface has reveled that the content of oxygen of different nature such as unidentate, bidentate and formation of bicarbonate species involved the surface hydroxyl groups.

The presence of superficial –OH on the catalyst has been reported to be important in the initial interaction of ethanol with these –OH groups to form ethoxy species [28] which could evolve to CH_3CHO, then this compound may either evolve over the surface

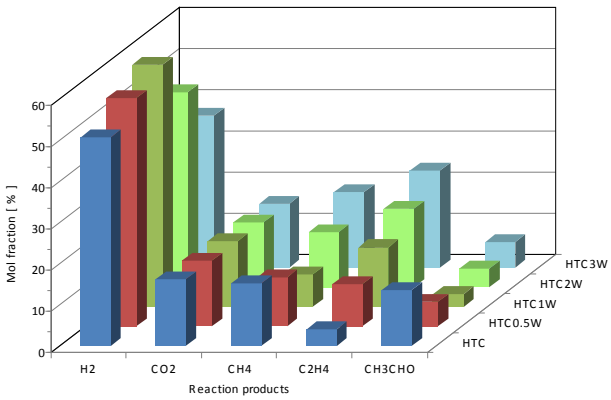

Figure 8. Reaction products from WOx/Co-Hydrotalcite catalysts evaluated at 450°C (7 h)

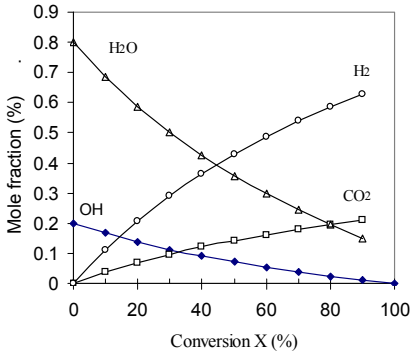

Figure 9. Mole fractions *y*i for each reaction product calculated from de Equation (9)

through alkyl elimination or form a bidentate acetate species, which suffers a C-C scission on the surface of the hydrotalcite producing CO_2, CH_4 and H_2 in the presence of water. This explanation could be similar for the steam reforming of ethanol using ZnO. This oxide has showed catalytic activity producing H_2, CO_2 and CH_3CHO [28].

The HTC catalyst showed a mole fraction to CH_3CHO of 15% but with the addition of W it decreased to less than 10%. An inverse behavior was observed with the C_2H_4, the addition of W in the HTC3W catalyst increased and its mole fraction was more than 20%.

The reaction products in Figure 8 are produced in accordance with the following reactions:

$$CH_3CH_2OH + 3H_2O \rightarrow 2CO_2 + 6H_2 \quad (1)$$

$$CH_3CH_2OH \rightarrow CH_3CHO + H_2 \quad (2)$$

$$CH_3CH_2OH + H_2O \rightarrow CO_2 + CH_4 + 2H_2 \quad (3)$$

$$CH_3CH_2OH \rightarrow CH_2{=}\ CH_2 + H_2O \quad (4)$$

$$CO + H_2O \rightarrow CO_2 + H_2 \text{ (water-gas shift reaction)} \quad (5)$$

$$CH_4 + H_2O \rightarrow CO + 3H_2 \quad (6)$$

$$CH_2 = CH_2 + 2\ H_2O \rightarrow CH_4 + CO_2 + 2H_2 \quad (7)$$

$$CH_3CHO + H_2O \rightarrow CH_4 + CO_2 + 2H_2 \quad (8)$$

The CH_3CHO production decreased as the W concentration increased and we found this product in all the catalysts studied suggesting that hydrotalcite surface acted as dehydrogenation catalyst according with the reaction (2). It can be observed that H_2 was the main product because several reactions contributed to its production (mainly reaction 1). We did not find CO in the products and the dehydration of ethanol to CH_2=CH_2, reaction (4) was strongly affected by the presence of W. The catalyst HTC3W showed the highest conversion. Ethylene and acetaldehyde are intermediate products formed from ethanol dehydration and dehydrogenation respectively, reaction (4) and reaction (2). In accordance with other authors these products promoted coke formation [29]. The yields of these products as a function of space time have a typical behavior of intermediate products.[30].

From all the samples, the HTC1W catalyst showed the highest selectivity to H_2 and the lowest production of CH_3CHO. The difference in H_2 production between this catalyst and the others was very small. The H_2 production comes from several reactions; dehydrogenation, water-gas shift conversion of CO and decomposition of oxygenated compounds. In this way, infrared studies [31] have showed that dehydrogenation of molecularly adsorbed ethanol was proposed as a key reaction step. The ethanol adsorbs molecularly to form hydrogen-bonded weakly adsorbed species and to produce strongly adsorbed molecular ethanol on the Lewis-sites of the support. It was found that high temperature treatment of the adsorbed species caused the formation of surface acetate species on the support. The presence of water lowered the temperature of the appearance of acetate species and increased the stability of monodentate ethoxide species. At high temperature the decomposition of ethoxide (at the metal/support interface) led to the formation of H_2 [31].

3.7. Mole fraction calculations

We calculated the mole fractions *y*i for each reaction product from the chemical equilibrium constant K [32] for the reaction (1)(Figure 9). In this way y_{CO2} means the mole fraction of the CO_2, y_{H2} is the mole fraction of hydrogen; y_{OH} is for ethanol and y_{H2O} for water. The initial molar flow of water fed to the reactor was 4 moles/min ($N_{H2O}°$) and for the initial molar flow of CH_3CHOH ($N_{OH}°$) was 1mole/min. In accordance with the equation of the equilibrium constant (K), we calculated de conversion X.

$$K = \frac{y_{CO_2}^2 y_{H_2}^6}{y_{H_2O}^3 y_{OH}} \quad (9)$$

The mole balance of the reaction (1) was as follows:

$$N_{OH} = (N_{OH}° - N_{OH}° X) \quad (10)$$

$$N_{CO2} = N_{OH}° 2X \quad (11)$$

$$N_{H2} = N_{OH}° 6 X \quad (12)$$

$$N_{H2O} = (N_{H2O}° - N_{OH}° 3X) \quad (13)$$

$$N = \text{Total mole flow} = N_{OH}° + 4N°_{OH}X + N_{H2O}° \quad (14)$$

The mole fractions were:

$$y_{OH} = (N_{OH}° - N_{OH}° X) / N \quad (15)$$

$$y_{CO2} = (N_{OH}° 2X) / N \quad (16)$$

$$y_{H2} = (N_{OH}° 6 X) / N \quad (17)$$

$$y_{H2O} = (N_{H2O}° - N_{OH}° 3X)/ N \quad (18)$$

The experimental and calculated mole fractions (or selectivity) for H_2, CO_2, H_2O were compared (Table 2) and small differences were found among the catalysts. These results suggested that these catalysts had high selectivity to H_2 and CO_2 and that HTC1W catalyst showed the highest H_2 mole fraction.

This catalyst with 1wt%W showed the lowest pore volume (Table 1) with a monomodal pore diameter distribution with 520 Å (Figure 2) and with a laminar structure typical of hydrotalcites where W^{6+} and Co ions have isomorphically replaced the Mg^{2+} cations in the brucite ($Mg(OH)_2$)-like layers (Figure 3). This catalyst showed an UV-vis spectrum that suggested the substitution of Co ions by W^{6+} ions (Figure 6) however this substitution was also observed in the other catalysts. The main difference of HTC1W catalyst with the HTC catalysts was the pore volume. This catalyst showed a pore volume of 0.47 cm^3/g (Table 1) against 0.86 cm^3/g of the HTC catalyst without W. It could be possible that ethanol molecules had long residence time in the small pore volumes increasing the H_2 and CO_2 selectivity but this hypothesis will be proved in a future work.

The H_2 and CO_2 mole fractions or selectivities for all the samples were close to the equilibrium. The presence of Co catalyzed the reaction to get high selectivities (near the equilibrium). The presence of W change the chemical properties of the Co-hydrotalcite surface, this conclusion was inferred from UV-vis spectra. W^{6+} ions were interacted with Al and Mg ions inside the lamellar structure of the hydrotalcites. This interaction increased the bond strength of Mg-O-W-O-Al- in a similar way as W-O-Al-bond in Al_2O_3 [9]. This promoter effect of W in the structure of the Co-hydrotalcite was more evident in the catalytic stability tests.

3.8. Catalytic Stability

The catalyst HTC1W (with 1 wt% W) showed a great stability after 7 h at 450°C (Figure 10) and it showed the highest production of H_2 (Figure 8). This behavior was very similar with the W effect in catalysts of Pt supported on Al_2O_3 [10,33]. In that study, low concentrations of tungsten oxides (below of monolayer, W< 1wt%) stabilized the Al_2O_3 and Pt particles. The sinterization process of Pt was reduced and the catalysts were active for a long time. In this study the addition of W to the Co-hydrotalcite produced more stability in function of reaction time.

Table 2. Experimental and calculated mole fractions of the reaction products for the WOx/Co- Hydrotalcite catalysts at 76% of conversion.

Catalyst	C_2H_5OH	H_2	CO_2	H_2O
	Experimental	Experimental	Experimental	Experimental
HTC	0.054	0.51	0.16	0.216
HTC05W	0.055	0.56	0.16	0.22
HTC1W	0.051	0.59	0.16	0.204
HTC2W	0.050	0.47	0.16	0.20
HTC3W	0.034	0.37	0.15	0.136
Calculated	0.024	0.57	0.19	0.19

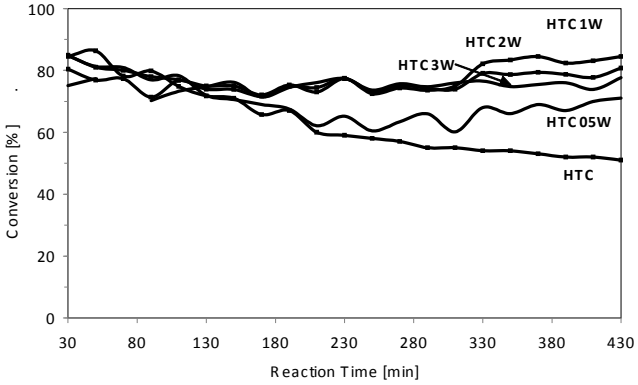

Figure 10. Deactivation tests of WOx/ Co-Hidrotalcites at 450°C

It was very evident that W^{6+} ions stabilized the Co-hydrotalcite structure at low concentration. The HTC catalyst without W showed a rapid deactivation in contrast with the HTC1W catalyst. It seemed that catalysts with the presence of Co domains stabilized with W^{6+} ions and with small pore volume produced catalytic sites able to make cracking or C-C bonds [18] with good performance to produce H_2.

4. CONCLUSIONS

Tungsten-Co-hydrotalcite catalysts showed porous with the shape of parallel layers with a monomodal mesoporous distribution. Superficial chemical groups as: -OH, H_2O, Al-OH, Mg-OH, -O-W-O and CO_3^{2-} were found by infrared spectroscopy. The absence of other phases by XRD suggested that both W^{6+} and Co have isomorphically replaced the Mg^{2+} cations in the brucite ($Mg(OH)_2$)-like layers. As W concentration increased, the intensity of crystalline reflections of the catalysts decreased. We did not find any tetrahedral or octahedral tungsten oxide compounds on the surface. By UV-vis spectroscopy the Co^{2+} ion was substituted by W^{6+} ions. It was found a promoter effect of W on the Co-hydrotalcite catalysts for the ethanol steam reforming. The addition of W in low amounts (1wt%W) produced great catalyst stability and high H_2 production. The catalysts did not produce CO and showed low production to CH_3CHO. These enhanced catalytic properties for the catalyst with 1wt%W were related with an excellent stabilization produced by the W^{6+} ions bonded with the Co-hydrotalcite structure and small pore volume.

5. ACKNOWLEDGEMENTS

The authors acknowledge the financial support of the Universidad Autónoma Metropolitana-Azcapotzalco, Iztapalapa, the Instituto Politécnico Nacional and the Instituto Mexicano del Petróleo.

REFERENCES

[1] R.D. Cortright, R.R. Davda, J.A. Dumesic, Nature, 418, 964 (2002).

[2] J. Llorca, N. Homs, J. Sales, J.L.G. Fierro and P. Ramírez de la Piscina, J. Catal., 222, 470 (2004).

[3] A. Aboudheir, A. Akande, R. Idem, A. Dalai, Int. J. of Hydrogen Energy, 31, 752 (2006).

[4] U.S. Ozkan and Kurt Koelling, Fuel Cell Grade Hydrogen Production from the Steam Reforming of Bio-Ethanol Over Co-based catalysts: An Investigation of Reaction Networks and Active Sites. Tesis, The Ohio State University (2005).

[5] M.A. Ortiz R., Hydrogen production from bio-ethanol using Co, Ni and Pt-hydrotalcite catalysts stabilized with WOx, Tesis UAM-Azcapotzalco, (2009).

[6] F. Trifiró, A. Vaccari in: A.G. Bein (Ed.), Comprehensive Supramolecular Chemistry, vol.7, Pergamon, New York, (1996) p.251.

[7] M.A. Ocaña Z., Síntesis de Hidrotalcitas y Materiales Derivados: Aplicaciones en Catálisis Básica. Ph.D. Thesis , Universidad Complutense de Madrid, (2005).

[8] J. Salmones, B. Zeifert, M.H. Garduño, J. Contreras L., D.R. Acosta, A. Romero S. and L.A. García, Catal. Today, 133, 886 (2008).

[9] F. Cavan, F. Trifiro, A. Vacari, Catal. Today, 11, 173 (1991).

[10]J.L.Contreras, G.A. Fuentes, J. Salmones, B. Zeifert, Stabilization of Supported Platinum/Gama-Alumina Catalysts by Addition of Tungsten, J. of Alloys and Compounds 483, 371 (2008).

[11]J.L. Contreras, J. Salmones, L.A. García, A. Ponce, B. Zeifert and G.A. Fuentes, Hydrogen production by etanol steam reforming over Co-hydrotalcites having basic sites. J. of New Materials for Electrochemical Systems 11, 109 (2008).

[12]M.N. Barroso, M.F. Gómez, L.A. Arrúa, M.C. Abello, Appl. Catal. A:General, 304, 116 (2006).

[13]J. Llorca, N. Homs, J. Sales, and P. Ramírez de la Piscina, J. Catal., 209, 306 (2002).

[14]S. Lowell, J.E. Shields, M.A. Thomas, and M. Thommes, Characterization of Porous Solid and Powders: Surface Area, Pore Size and Density, Kluwer Academic Publischers, 2004.

[15]M. Arco, D. Carriazo, s. Gutiérrez, C. Martín and V. Rives, Inorg. Chem. 43, 375 (2004).

[16]I.O. Cruz, N.F.P. Ribeiro, D.A.G. Aranda, M.M.V.M. Souza, Catalysis Comm. 9, 2606 (2008).

[17]T. Shishido, M. Sukenobu, H. Morioka, R. Furukawa, H. Shirahase, K. Takehira, Catal. Lett., 73, 8, 21 (2001).

[18]C. Resini, T. Montenari, L. Barattini, G. Ramis, G. Busca, S. Presto, P. Riani, R. Marazza, M. Sisani, F. Marmottini, U. Costantino, Appl. Catal.A: General, 355, 83 (2009).

[19]J.M. Stencel, "Raman Spectroscopy for Catalysis", Van Nostrand Reinhold, New York (1990) 82-85.

[20]R.H. Busey and O.L. Keller Jr., J. Chem. Phys., 41, 215 (1964).

[21]A. Bartecki and Dembicka D., J. of Inorg. and Nuclear Chem., 29, 2907 (1967).

[22]J.L.Contreras and G.A. Fuentes, Studies in Surface Science and Catalysis, Vol. 101 Edit. B. Delmon and J.T. Yates, Elsevier (1996) 1195-1204.

[23]A. Iannibello, L. Villa, and S. Marengo, Gazzetta Chimica Italiana,109, 521 (1979).

[24]L. Salvati, L.E. Makovsky, J.M. Stencel, F.R. Brown, D.M. Hercules, J. Phys.Chem., 85, 3700 (1981).

[25]J.A. Horsley, I.E. Wach, J.M. Brown, G.H. Via, F.D. Hardcastle, J. Phys. Chem., (1987).

[26]W.P. Griffith and T.D. Wickins, J. Chem. Soc., A, 1087 (1966).

[27]J.R. Anderson and K.C. Pratt, Introdution to characterization and testing of catalysts, Academic Press, (1985), p.419-420.

[28]J. Llorca, N. Homs, P. Ramírez de la Piscina, J. of Catal., 227, 556 (2004).

[29]J.R. Rostrup-Nielsen, N. Hojlund in: J. Oudar, H. Wise (Eds.), Deactivation and Poisoning of Catalyst, Marcel Dekker, New York, Basel, 1985,p.57.

[30]J. Comas, F. Mariño, M. Laborde, N. Amadeo. Chem. Eng., J., 98, 61 (2004).

[31]A. Erdohelyi, J. Rasko, T. Kecskes, M. Toth, M. DömÖk, K. Baán, Catal. Today, (2006).

[32]J.M. Smith, Chemical Engineering Kinetics, Spanish Ed. P.36 (2001).

[33]J.L. Contreras, G.A. Fuentes. J. Salmones, B. Zeifert. Effect of the reduction temperature of Pt/WOx-Al_2O_3 catalysts upon n-heptane hydroconversion. Proceedings of the ISAHOF meeting , Ixtapa-Zihuatanejo, México, Jun.14-18 ,2009.